A Fast Image Matching Algorithm Using a Combination of Line Segment Features

FU Runzhe[1], *LENG Xuefei*[1*], *ZHU Yiming*[2], *LIU Rui*[1], *HAO Xiang*[1]

1. College of Astronautics, Nanjing University of Aeronautics and Astronautics, Nanjing 210016, P.R. China;
2. Tandon School of Engineering, New York University, New York 11201, USA

(Received 27 February 2020; revised 12 May 2020; accepted 20 July 2020)

Abstract: The scene matching navigation is a research focus in the field of autonomous navigation, but the real-time performance of image matching algorithm is difficult to meet the needs of real navigation systems. Therefore, this paper proposes a fast image matching algorithm. The algorithm improves the traditional line segment extraction algorithm and combines with the Delaunay triangulation method. By combining the geometric features of points and lines, the image feature redundancy is reduced. Then, the error with confidence criterion is analyzed and the matching process is completed. The simulation results show that the proposed algorithm can still work within 3° rotation and small scale variation. In addition, the matching time is less than 0.5 s when the image size is 256 pixel×256 pixel. The proposed algorithm is suitable for autonomous navigation systems with multiple feature distribution and higher real-time requirements.

Key words: image matching; navigation; Hough transform; Delaunay triangulation; combined feature

CLC number: TN967.2 **Document code:** A **Article ID:** 1005-1120(2021)03-0501-11

0 Introduction

Image matching is a process of matching operations between reference images and measured images. With the development of image sensors and computer vision technology, the image matching technology is widely used in aircraft navigation, augmented reality, pattern recognition and other fields. In the field of navigation, using image navigation has a greater advantage in acquiring information than other methods (e.g. inertial navigation, GPS navigation)[1], so the scene matching navigation is widely used in aerospace navigation, intelligent robots and military applications[2]. And the research of image matching algorithm has great significance for the development of autonomous navigation.

Image matching algorithms can be roughly classified into gray-based[3-5] and feature-based[6-7] matching methods. In the navigation process, the algorithm based on gray-scale correlation is not fully applicable, because the result of image matching is limited by the shooting conditions and time constraints, and the pre-stored map in navigation system has certain gray-scale and geometric deformation differences with the actual aerial image. The feature-based matching algorithm is generally robust to illumination changes, rotation and even scale changes of scenes in the image, so it is more suitable for autonomous navigation. The feature-based matching algorithm first extracts the features in the image, and then establishes the correspondence between the two images. The difficulty of this method lies in the automatic, stable and consistent feature extraction and matching process. At the same time, in the case of navigation, there is also a high demand for real-time image matching[8]. Lowe[9] proposed the scale-invariant feature transform (SIFT) matching algorithm, which has good performance against rotation and scale change, so it has received extensive attention. However, the SIFT feature extraction process is time consuming and difficult to

*Corresponding author, E-mail address: lengxuefei@nuaa.edu.cn.

How to cite this article: FU Runzhe, LENG Xuefei, ZHU Yiming, et al. A fast image matching algorithm using a combination of line segment features[J]. Transactions of Nanjing University of Aeronautics and Astronautics, 2021, 38(3): 501-511.
http://dx.doi.org/10.16356/j.1005-1120.2021.03.014

meet navigation requirements. Bay et al.[10] proposed the speeded-up robust features (SURF) algorithm. Its feature point detection theory is also based on the scale space and is robust to illumination. The calculation speed of the SURF algorithm is about three times that of the SIFT algorithm. However, when using the SURF algorithm to match the feature point, mismatching points is easy to occur. At present, many domestic and foreign researchers are working to solve this problem. In 2011, Rublee et al.[11] proposed an algorithm for fast feature point extraction and description called ORB (Oriented FAST and rotated BRIEF), which combines the FAST feature extraction algorithm and the BRIEF feature description algorithm to greatly improve the operation speed. However, this algorithm is not robust to the case of scale transformation. In addition, its fuzzy robustness and rotational robustness are slightly weaker than the SURF algorithm. In the actual navigation environment, especially in urban areas, there are many feature points in the background. These feature points produce huge amount of data calculation, which will seriously slow down the running speed of matching process. Under such a huge amount of computation, even the fast ORB algorithm is also difficult to meet navigation needs. Therefore, the research of image matching algorithm has its particularity in the field of autonomous navigation.

In order to meet real-time requirements, domestic and foreign scholars try to use line features for image processing. Zhang et al.[12] proposed a fast and high-precision image matching method based on the Edline line features. Wu[13] proposed a plane tracking algorithm based on edge matching for the planar target tracking problem of video mobile pilot. Chen et al.[14] applied the line segment matching method to the three-dimensional reconstruction of unmanned aerial camera imaging. Cao et al.[15] used the line feature to optimize the 3D model, improved the visual effect of the model, and maintained the plane and edge features of the 3D model. Konovalenko et al.[16] applied linear extraction to the background of drone navigation and achieved good experimental results. Kunina et al.[17] used the Hough transform to extract the straight line in the image and fit it with least squares method, and combined the RANSAC algorithm to use the line feature in UAV image navigation. Wu et al.[18] used a new method of line detection, which directly carried out contour difference in the image plane to enhance the robustness to noise and blur. Although the line segment feature can greatly reduce the feature density, the line segment extraction algorithm still has problems such as low extraction precision. Its matching accuracy is less than the traditional point feature algorithm. In practical applications, the improvement and combination of line segment feature and point feature algorithm have important research value and significance.

This paper improves the Hough transform and the Delaunay triangulation algorithm, and proposes a fast matching algorithm based on the line segment combination feature, in order to improve the accuracy and robustness, and to meet real-time requirements of autonomous navigation system in image matching technology. The simulation results show that the proposed algorithm not only simplifies the redundancy features, but also improves its accuracy compared with the traditional line feature extraction. Besides, it has good real-time performance, which can meet the specific requirements of the image matching algorithm in autonomous navigation system.

1 Line Segment Feature Extraction and Improved Method Based on Hough Transform

1.1 Principle of Hough transform

The Hough transform is a feature extraction technique in image processing. It can be used to detect lines and curves in the images[19]. The core idea is the transformation of the coordinate system.

The Hough transform is concerned with identification of lines. It determines whether the edge points formed a straight line by detecting the line family function of these points and counting the number of corresponding intersecting sinusoids in the polar coordinate system. On the basis of the

above, the progressive probabilistic Hough transform (PPHT) uses a random extraction point and sets the accumulator to determine the line, which speeds up the operation[20].

1.2 Improved line segment feature extraction algorithm

The probabilistic Hough transform is used to extract line segments in the edge binary map[21]. Then a threshold is used to eliminate very short line segments. The threshold should be determined by the specific matching image size and feature distribution. In this way, lines l_1, l_2, $\cdots$, l_t are obtained. After that, the corresponding midpoints (p_1, p_2, $\cdots$, p_t) of each line segment are extracted in turn. The next step is to calculate the coordinates of the corresponding midpoints ($p_1(x_1, y_1)$, $p_2(x_2, y_2)$, $\cdots$, $p_t(x_t, y_t)$) and dip angles relative to the horizontal line of the image (α_1, α_2, $\cdots$, α_t). Since the Hough transform may have certain errors in the calculation process, in order to reduce the calculation error, several points at both ends of the line segment can be selected to calculate the midpoint coordinates and the line segment inclination. In this paper, for each line segment, take five points at both ends of the line segment. Taking the line segment l_1 as an example, the five points are $o_{i1}(x_1, y_1)$, $o_{i2}(x_2, y_2)$, $\cdots$, $o_{i(n-1)}(x_{n-1}, y_{n-1})$, $o_{in}(x_n, y_n)$. All the points on the line can be extracted by the polar feature conversion process of edge binary image. The transform is implemented by quantizing the Hough parameter space into finite intervals or accumulator cells. Specific implementation principles are shown in Ref.[20]. Since the minimum line length threshold is 20 in the test, there is no case of $n-5\leqslant 5$, that is, the point distribution used for calculation is selected on both sides of the line segment, as shown in Fig.1.

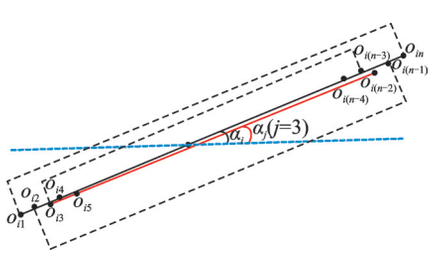

Fig.1 Schematic diagram of calculation of line segment information

Let

$$x_i = \frac{1}{5}\sum_{j=1}^{5}(x_{n-j+1} + x_j) \tag{1}$$

$$y_i = \frac{1}{5}\sum_{j=1}^{5}(y_{n-j+1} + y_j) \tag{2}$$

where (x_i, y_i) is the coordinates of the midpoint of the line segment.

In the schematic diagram, α_i represents the angle between the current black line segment and the horizontal axis of the image coordinate system. And the dip angle α_i is calculated as follows

$$\alpha_i = \frac{1}{5}\sum_{j=1}^{5}\alpha_j \tag{3}$$

where α_j is the angle between the horizontal axis and the line connected by the jth and the $(n-j+1)$th point. For example, when $j=3$ in Fig.1, α_j represents the angle between the horizontal axis, which is marked with blue dotted line, and the red line, which connects the 3rd point and the third last point. Calculation of α_j is expressed as

$$\alpha_j = \arctan\frac{y_{n-j+1} - y_j}{x_{n-j+1} - x_j} \tag{4}$$

Traverse the information of all the line segments, and detect the difference between their distances and difference between dip angles. Use the distance from a midpoint of the line segment to the other line segment to describe the distance $s_{k,l}$ ($1\leqslant k\leqslant t, 1\leqslant l\leqslant t, k\neq l$) between two line segments. For two line segments, when the differences of their dip angles and distances are less than a given threshold, they are judged as one straight line. The weighted average value of various information of the line segments replaces their true values, and the weight is the length of the extracted line segment. For example, when two straight lines l_1, l_2 are satisfied with Eqs.(5,6), those two line segments are determined as the same line segment.

$$s_{1,2} = \frac{|Ax_1 + By_1 + C|}{\sqrt{A^2 + B^2}} < \sigma_1 \tag{5}$$

$$|\alpha_1 - \alpha_2| < \sigma_2 \tag{6}$$

where σ_1 and σ_2 are set thresholds, (x_1, y_1) and (x_2, y_2) the midpoint coordinates corresponding to the line segment, α_1 and α_2 the dip angles of line segments, and A, B and C the linear equation parameters of l_2, which satisfy $Ax_2 + By_2 + C = 0$. Com-

bine the two line segments to get the new line segment l_{new} with parameters as follows

$$x_{new} = \frac{k_1 x_{1+} k_2 x_2}{k_1 + k_2} \tag{7}$$

$$y_{new} = \frac{k_1 y_{1+} k_2 y_2}{k_1 + k_2} \tag{8}$$

$$\alpha_{new} = \frac{k_1 \alpha_{1+} k_2 \alpha_2}{k_1 + k_2} \tag{9}$$

$$k_{new} = s_{1,2} + \frac{k_1 + k_2}{2} \tag{10}$$

where k_1, k_2 and k_{new} represent the length of line segment l_1, l_2 and l_{new}, respectively; α_1, α_2 and α_{new} represent the dip angles of l_1, l_2 and l_{new}, respectively. (x_{new}, y_{new}) represents the coordinate of new midpoint. After the above calculation, although (x_{new}, y_{new}) is not the real midpoint, this weighted averaging method preserves the geometrical characteristics of the feature distribution and makes it easier to construct subsequent combinations of features.

1.3 Feature extraction experiments

The simulation experiment is carried out using the improved feature extraction algorithm, and compared with the traditional Hough transform line extraction algorithm. The results are shown in Figs.2—5.

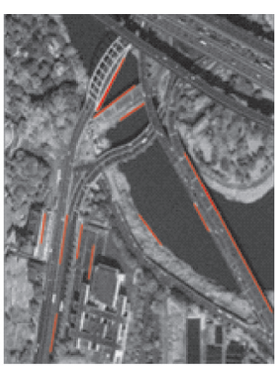

(a) Feature extraction of the reference map

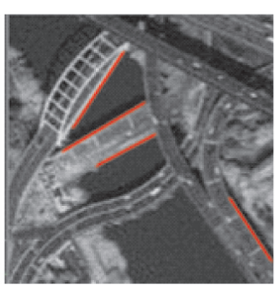

(b) Feature extraction of real-time graphs

Fig.2 Simulation results of improved line segment extraction algorithm

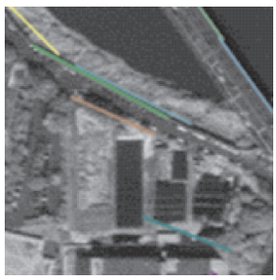

Fig.3 Error extraction in the traditional algorithm where the edge is too wide

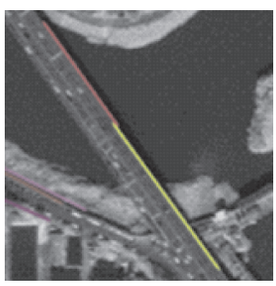

Fig.4 Error in extracting line segment breaks in traditional algorithms

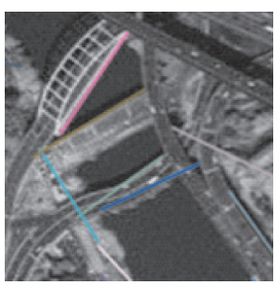

Fig.5 Error extraction in traditional algorithm where curve is defined as line segment

From Figs.2—5 we can see that:

(1) These simulation results show that using the traditional Hough transform algorithm to extract lines often causes extraction abnormalities.

(2) If extracting an edge which is too wide, we may get several very close edges. These edges are incorrect extraction results. As shown in Fig.3, the upper side edge of the riverside road is extracted as two line segments (marked by green and cyan line segments respectively).

(3) In noisy environment, segments extracted from long edges often break to several parts. As shown in Fig.4, the edges of the bridge break into two segments marked by yellow and purple during the extraction process.

(4) Fig.5 is a curve with a large arc at the edge

of the scene. This kind of curves is sometimes recognized as edges due to the algorithm error, which will cause matching error. As shown in Fig. 2, the blue and green line segments are extracted in error.

Therefore, the experimental results prove that the proposed line segment extraction algorithm can reduce the error extraction above effectively.

2 Combined Feature Descriptor Based on Delaunay Triangulation

In order to improve the accuracy of line segments matching and to construct robust features, we introduced the Delaunay triangulation to describe the geometric relationship between line segments. We further propose the matching for combined features based on line segment features. The schematic diagram of the combined features is shown in Fig.6.

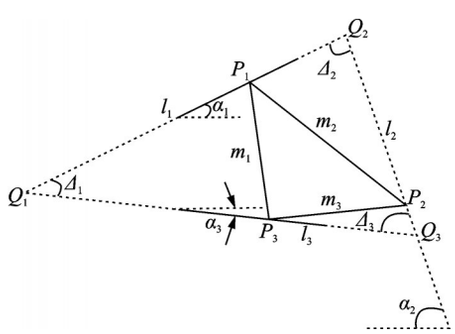

Fig.6 Schematic diagram of combined features

In Fig.6, α is the angle between the characteristic line segment and the horizontal axis of the image, and $\alpha \in [-90, 90]$. When the left end of the line segment is lower than the right end, α is defined as a positive value, and when the left end of the line segment is higher than the right end, α is negative.

Regard the midpoints of the obtained line segments as vertexes and use these vertexes to construct the Delaunay triangulation[22]. As shown in Fig.6, each side of the triangular mesh is marked as m_1, m_2, m_3, respectively. The extended lines of each edge line segment intersect at Q_1, Q_2, Q_3. Connect these three points and then get three lines l_1, l_2 and l_3. α_1, α_2, α_3 are the angles between horizontal line and l_1, l_2 and l_3, respectively. We define these angles as the basic matching element Δ_i.

$$\begin{cases} \Delta_1 = |\alpha_1 - \alpha_3| \\ \Delta_2 = |\alpha_2 - \alpha_1| \\ \Delta_3 = |\alpha_3 - \alpha_2| \end{cases} \tag{11}$$

Each Delaunay triangle contains three elements Δ_i (i=1, 2, 3), and Δ_1, Δ_2, Δ_3 form a three-dimensional combined feature $\boldsymbol{S}$. According to the method, traversing the midpoints of all the line segments can get several combined features $\boldsymbol{S}_1$, $\boldsymbol{S}_2$, $\cdots$, $\boldsymbol{S}_n$.

The combined feature $\boldsymbol{S}$ contains the angle information of the three segments, which have the specific geometric relationship, and the line intersection information of their extension line (Q_1, Q_2, Q_3 shown in Fig.6). The combined features obtained by directly searching for every three straight lines and the combined feature map obtained by the Delaunay triangulation are shown in Fig.7 and Fig.8, respectively. It can be seen that the method based on the Delaunay triangulation reduces the computational complexity for describing the geometric relationship of the line segments, and avoids a lot of repeated description.

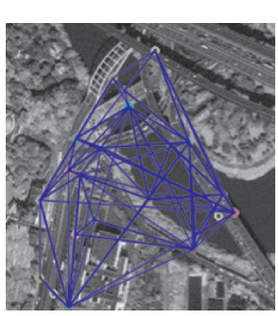

Fig.7 Combined features obtained by directly searching for every three straight lines

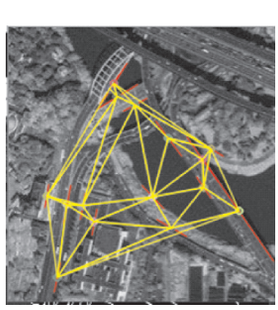

Fig.8 Combined feature map obtained by Delaunay triangulation

Moreover, because the Delaunay triangle network has good characteristics such as stability and disjointness, local errors have the least impact on the overall network. Compared with the fully-connected triangular network, the Delaunay triangulation can improve the stability of matching.

3 Matching Algorithm for Combined Features

For each matched combined features, there are three sets of matching segments as elements of image matching. In addition, the intersection point coordinate $p_t(x, y)$ of the extension line corresponding to the combined features can be obtained by simple geometric calculation. These intersections can also be used as the elements required for matching, and the confidence of each coordinate corresponds to its corresponding angle Δ_t, i.e. $V_t = \dfrac{1}{(\csc\Delta t)^2}$. Under the same error, the closer to 90° the angle Δ is, the smaller the position error ε_2 of the intersection of the line extension lines is. Therefore, under the same matching threshold, when Δ is closer to 90°, the confidence of the intersection coordinate matching is higher. Proof is shown in Fig.9.

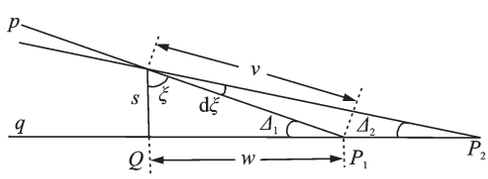

Fig.9 Schematic diagram of error analysis

As shown in Fig.9, the lines p, q intersect at point P_1, and the intersection angle is Δ_1. Due to the error in line segment extraction, p has an error dip $\mathrm{d}\xi$ with respect to q. Note the center of rotation as O, and Q is the perpendicular foot of the straight line p perpendicular to O. And note the length of OQ as s, and the length of QP changes with the change of error angle ξ. The lengths of OP and QP are denoted as variable v, w. The two straight lines actually intersect at point P_2 with an angle Δ_2. According to the geometric relationship of the combined features, the angle Δ of the straight line ranges from [0°, 180°], and we also get that

$$v = \frac{s}{\cos\xi} \tag{12}$$

$$w = s \times \tan\xi \tag{13}$$

$$\Delta = \arctan\frac{s}{w} \tag{14}$$

From Eqs.(12—14), the offset error ε of the line intersection P can be calculated as

$$\varepsilon = \mathrm{d}(s \times \tan\xi) = s \times (\sec\xi)^2 \mathrm{d}\xi - s \times (\csc\Delta)^2 \mathrm{d}\Delta \tag{15}$$

The curve of error function ε-Δ is shown in Fig.10.

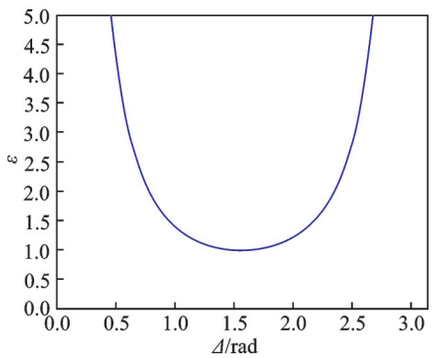

Fig.10 Curve of error function ε-Δ

From the error function, it can be concluded that the position error ε of the line intersection point takes the minimum value at $\Delta = \pi/2$, that is, under the same extraction error, the closer to the perpendicular the two lines are, the smaller the position error of the intersection point is, and the higher the confidence is.

Sort the angles stored in each of the two combined features $\boldsymbol{S}_i$ of the two images A and B to be matched . Then select the angle closest to 90° as the largest feature element $\Delta_{i\mathrm{Max}}$, which satisfies $|90° - \Delta_{i\mathrm{Max}}| = \min\{|90° - \Delta_j|\}$, j=1, 2, 3; And select the angle closest to 0° or 180° as the smallest feature element $\Delta_{i\mathrm{Min}}$, which satisfies $|90° - \Delta_{i\mathrm{Min}}| = \max\{|90° - \Delta_k|\}$, k=1, 2, 3. The last remaining element is marked as $\Delta_{i\mathrm{Mid}}$, and each element is marked with its corresponding confidence V^A_{Max}, V^A_{Min}, V^A_{Mid}, V^B_{Max}, V^B_{Min}, V^B_{Mid}, which satisfy with that

$$\begin{cases} V^A_{\mathrm{Max}} > V^A_{\mathrm{Mid}} > V^A_{\mathrm{Min}} \\ V^B_{\mathrm{Max}} > V^B_{\mathrm{Mid}} > V^B_{\mathrm{Min}} \end{cases} \tag{16}$$

Next, traverse through the elements $\Delta^A_{i\mathrm{Max}}$, $\Delta^A_{i\mathrm{Min}}$, $\Delta^A_{i\mathrm{Mid}}$, $\Delta^B_{j\mathrm{Max}}$, $\Delta^B_{j\mathrm{Min}}$, $\Delta^B_{j\mathrm{Mid}}$ in each combined fea-

ture, $\boldsymbol{S}_i^A$, $\boldsymbol{S}_i^B$. When we have

$$\left|\Delta_{it}^A - \Delta_{ju}^B\right| \leqslant \varepsilon_1 \tag{17}$$

it shows that Δ_{it}^A matches with Δ_{ju}^B, and then the mean of the confidence of the two elements is taken as

$$V_k = (V_{it}^A + V_{ju}^B)/2 \tag{18}$$

In Eqs.(17,18), ε_1 is the threshold set according to the experimental requirements, t and u represent any one of the subscripts Max, Min, Mid, and k=1, 2, 3 records three comparison processes. If the three angles of a combined feature match, three confidence mean values are accumulated. If the accumulated total confidence is bigger than the set threshold V_0, i.e. $\sum_{k=1}^{3} V_k > V_0$, the combined features can be considered to match. In this experiment, ε_1=1.5, V_0=1.1, confidence $V_t = 1/(\csc\Delta_t)^2$.

In general, the steps of the matching process are as follows:

(1) For each combined feature $\boldsymbol{S}$, get matching elements Δ_{Max}, Δ_{Mid} and Δ_{Min} and corresponding confidences V_{Max}, V_{Mid} and V_{Min}.

(2) Calculate the interpolation of matching elements in two combined features using Eq.(17). If Eq.(17) is satisfied for all three pairs of matching primitives, use Eq.(18) to average the three pairs of confidences V_1, V_2 and V_3. If Eq.(17) is not satisfied, compare other feature pairs.

(3) Add up V_1, V_2 and V_3. If the accumulated total confidence is bigger than the set threshold V_0, i.e. $\sum_{k=1}^{3} V_k > V_0$, the combined features can be considered to match.

The flow chart of the matching algorithm is shown in Fig.11. Experiment results of the matching algorithm are shown in Figs.12—14, where red lines represent the extracted line feature, yellow lines describe the Delaunay triangle network constructed by our algorithm, and purple lines are the extension cords of the line feature. The line segment extension line in each combination feature is compared with the cyan point, which shows the angle information in the combined features. These angles correspond to Δ_1, Δ_2 and Δ_3 in each combined fea-

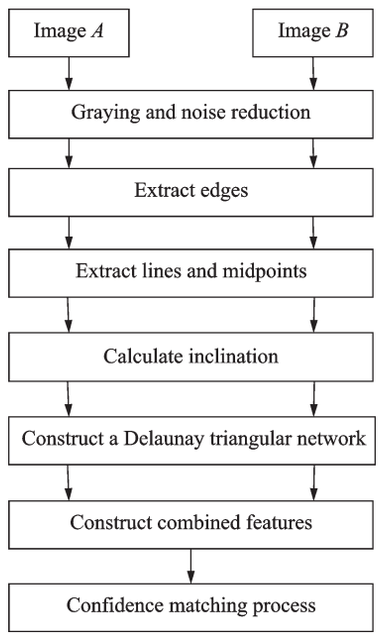

Fig.11 Flow chart of proposed algorithm

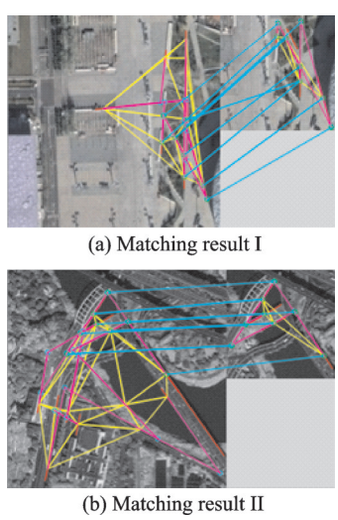

(a) Matching result I

(b) Matching result II

Fig.12 Matching results of optical image

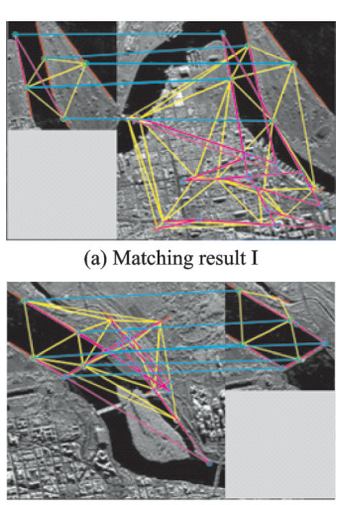

(a) Matching result I

(b) Matching result II

Fig.13 Matching results of synthetic aperture radar image

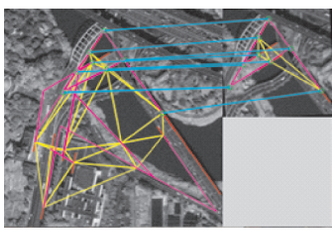

Fig.14 Matching result when image has a 3° rotation

ture $\boldsymbol{S}$. Particularly, some of the extension line intersections beyond the portion of the image are not drawn in the image, but they still participate in the matching process.

4 Simulation Results and Analysis

In order to verify the effectiveness of the proposed algorithm, the experiment is performed on a PC with a frequency of Intel CORE(TM) i5-3337U 1.8 GHz and 12 GB memory. The program development environment is Visual Studio 2013. In the experiment, the two matched images are 256 pixel×256 pixel and 128 pixel×128 pixel, respectively, and the minimum length threshold of the line segment extraction is 20. Constraint parameters for line segment screening are set as $\sigma_1=2.5°$, $\sigma_2=3°$, matching threshold $\varepsilon_1=1.5$, $V_0=1.1$. Multiple sets of experiments are performed with image shifting, small amplitude rotation and scaling, and the results are compared with the results from the SIFT and ORB algorithms.

Table 1 shows the averages of matching results in different images and transformation situation. Table 2 shows the comparison results of three algorithms. Results show that the proposed algorithm can effectively extract combined feature information from images, and also be able to maintain the matching accuracy with certain rotation and scaling. According to the experimental situation, the upper limit of rotation is 5°, the upper and the lower scaling limits are 2 and 0.7 times. Once these limits are exceeded, the extracted features could not be matched correctly and effectively. But the run time of the proposed algorithm is much faster than that of the traditional algorithms, which can meet navigation needs better. According to these characteristics of the proposed algorithm, it can be applied to the scene navigation task based on sequence image, which requires the used algorithm be robust to small amplitude rotation and scale change. However, the proposed algorithm still needs to be improved to adapt to more strict conditions.

Table 1 Matching results in different images and transformation situation

Number of features in the pre-stored graph	Number of features in the real-time graph	Rotation angle/(°)	Scale change/ times	Matching error/pixel	Run time / s
57	12	0	0.00	0.852 8	0.218
54	24	0	0.00	0.915 0	0.410
48	8	3	0.00	1.347 8	0.281
57	6	0	0.97	1.086 1	0.227
54	16	1	1.02	1.547 1	0.328

Table 2 Comparison results of three algorithms

Algorithm	SIFT	ORB	Proposed
Run time / s	1.485	0.442	0.223
Number of features (pre-stored graph)	990	442	57
Number of features (real-time graph)	260	197	14

To further show the advantages of the proposed algorithm, the comparison of features between SIFT, ORB and the proposed algorithms is shown in Fig.15.

According to the above results, the matching time of the proposed algorithm is basically distributed in the period of 0.2—0.5 s. The calculation speed of the proposed algorithm is faster than those of ORB and SIFT algorithms. In addition, the feature distribution of the proposed algorithm is more uniform than that of the ORB algorithm, and in the

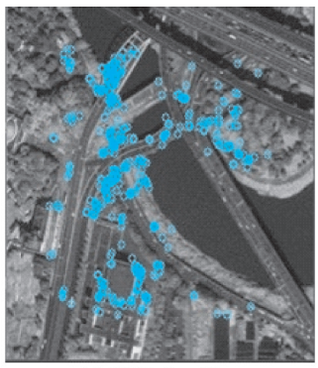

(a) ORB algorithm

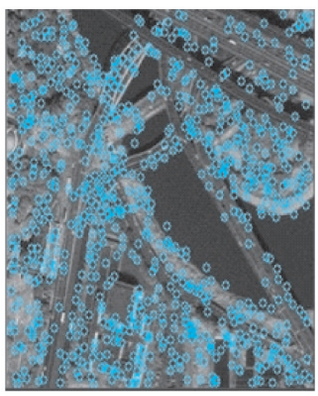

(b) SIFT algorithm

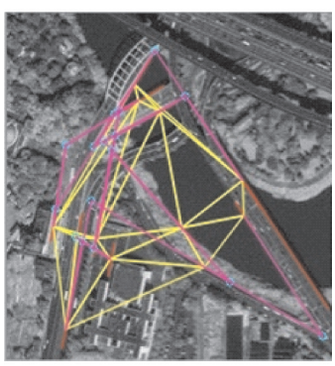

(c) Proposed algorithm

Fig.15 Feature quantity comparison of three algorithms

case of a large amount of feature information, the proposed algorithm can reduce redundant information and ensure matching speed. Besides, the matching accuracy is kept within 1.5 pixels, and the matching accuracy can be ensured under the condition of 3° rotation and small amplitude scale variation. Results show that the proposed algorithm has certain robustness and high accuracy, and is applicable for the case where the feature distribution is large and the matching speed is required.

5 Conclusions

A fast matching algorithm based on line segment geometry is proposed. Based on the Hough transform, the line segment features are searched, and the Delaunay triangulation method is introduced to combine the point and line features to realize the searching and matching process. Experiments show that the algorithm can reduce feature information redundancy and has good robustness and accuracy. In addition, the algorithm has good real-time performance and high speed to meet navigation and positioning requirements. However, there are still some improvements in the algorithm. For example, we need consider how to overcome the inaccuracy of line segment extraction and line segmentation ambiguity, and how to extend the scope of the method.

References

[1] LIU Chenfan. Overview of scene matching navigation[C]//Proceedings of the 8th China Satellite Navigation Conference. Shanghai, China: [s.n.], 2017: 83-87. (in Chinese)

[2] LI Yubo. Research on visual odometry for mobile robot in outdoor environment[D]. Changsha: National University of Defense Technology, 2012. (in Chinese)

[3] LI Tie, FU Yuanyuan, ZHANG Chi, et al. Research on gray scale face image matching algorithm based on invariant moment theory[J]. Computer Knowledge and Technology, 2018,14(28):189-190. (in Chinese)

[4] ZHU Wanyi, MU Pingan, DAI Muguang. Detection of transparent lamp parts based on image matching[J]. Acta Metrologica Sinica, 2018,39(3): 353-358. (in Chinese)

[5] FAN Xu, CAO Zhongqing. Image matching approach based on grey relational analysis and wind driven optimization[J]. Computer Engineering and Design, 2018, 39(8): 2598-2602. (in Chinese)

[6] SCHMID K, LUTZ P, TOMIC T. Autonomous vision-based micro air vehicle for indoor and outdoor navigation[J]. Journal of Field Robotics, 2014, 31(4): 537-570.

[7] YU Yang, XIAO Yang, REN Fangyu, et al. Survey of image extraction and registration based on OpenCV and remote sensing images[J]. Science and Technology Innovation Herald, 2018, 15(10): 48-49. (in Chinese)

[8] GONG Zhe. Research on the key technology for sequence image matching aided navigation system based on high-dimensional combined feature[D]. Nanjing:

Nanjing University of Aeronautics and Astronautics. (in Chinese)

[9] LOWE D G. Object recognition from local scale-invariant features[C]//Proceedings of the International Conference on Computer. Corfu, Greece: [s. n.], 1999, 2: 1150-1157.

[10] BAY H, ESS A, TUYTELAARS T, et al. Herbert bay speeded-up robust features(SURF)[J]. Computer Vision and Image Understanding, 2008, 110(3): 346-359.

[11] RUBLEE E, RABAUD V, KONOLIGE K, et al. ORB: An efficient alternative to SIFT or SURF[C]//Proceedings of the IEEE International Conference on Computer Vision. Barcelona, Spain: IEEE, 2011: 2564-2571.

[12] ZHANG Zhen, WANG Yongxiong. Fast image matching algorithm based on Edline line features[J]. Computer and Digital Engineering, 2019, 47(3): 652-656. (in Chinese)

[13] WU Yu. Plane target tracking based on edge matching[J]. Modern Computer, 2019(6): 68-71. (in Chinese)

[14] CHEN Qifeng, LIU Jun, LI Wei, et al. Line matching in three-dimensional reconstruction[J]. Journal of Wuhan Institute of Technology, 2018, 40(4): 446-450. (in Chinese)

[15] CAO Lin, WANG Guangxia, WANG Weiqi, et al. A 3D model optimization method based on oblique image line feature[J]. Journal of Nanjing University of Aeronautics & Astronautics, 2020, 52(6): 980-988. (in Chinese)

[16] KONOVALENKO I, KUZNETSOVA E, MILLE A, et al. New approaches to the integration of navigation systems for autonomous unmanned vehicles (UAV)[J]. MDPI-Sensors, 2018(18): 3010-3033.

[17] KUNINA I A, TEREKHIN A P, KHANIPOV T M, et al. Aerial image geolocalization by matching its line structure with route map[C]//Proceedings of the 9th International Conference on Machine Vision (ICMV). Nice, France: [s.n.], 2016: 2A1-2A7.

[18] WU Jian, DENG Mengwei, ZHONG Peihua. A line detection algorithm using contour difference[J]. Data Acquisition and Processing, 2020, 35(6): 1182-1191. (in Chinese)

[19] DUDA R O, HART P E. Use of the Hough transformation to detect lines and curves in pictures[J]. Communications of ACM, 1972, 15: 11-15.

[20] MAO Xingyun, LENG Xuefei. Getting started with OpenCV3 programming[M]. Beijing: Publishing House of Electronics Industry, 2018. (in Chinese)

[21] HU Bin, ZHAO Chunxia. A fast lane detection method based on the progressive probabilistic Hough transform[J]. Microelectronics & Computer, 2011, 28(10): 177-180. (in Chinese)

[22] WANG Chongchang, HAN Xu. Image segmentation based on Delaunay triangulation expression[J]. Geomatics & Spatial Information Technology, 2019, 42(3): 216-221. (in Chinese)

Acknowledgement This work was supported by the Fundation of Graduate Innovation Center in Nanjing University of Aeronautics and Astronautics (No.kfjj20191506).

Authors Mr. **FU Runzhe** received the B.S. degree in navigation guidance and control from Nanjing University of Aeronautics and Astronautics and received the B.S. degree in aircraft avionics technician from Ukraine National Aerospace University in 2017. He is currently studying for the master's degree in College of Astronautics, Nanjing University of Aeronautics and Astronautics. His research interest is scene matching navigation.

Dr. **LENG Xuefei** received the B.S. and the Ph.D. degrees in measurement and control technology and instrumentation program from Nanjing University of Aeronautics and Astronautics in 2000 and 2007, respectively. She joined in Nanjing University of Aeronautics and Astronautics in June 2007, where she is an associate professor of College of Astronautics. Her research is focused on integrated navigation system and image processing fields.

Author contributions Mr.**FU Runzhe** designed the study, complied the models, conducted the analysis, interpreted the results, and wrote the manuscript. Dr.**LENG Xuefei** gave guidance on direction guidance and experimental protocols. Mr.**LIU Rui**, Mr.**ZHU Yiming** and Mr.**HAO Xiang** contributed to the discussion and background of the study. All authors commented on the manuscript draft and approved the submission.

Competing interests The authors declare no competing interests.

(Production Editor: ZHANG Huangqun)

结合线段组合特征的快速图像匹配算法

付润喆[1]，冷雪飞[1]，朱一鸣[2]，刘 瑞[1]，郝 祥[1]

（1.南京航空航天大学航天学院，南京 210016，中国；2.纽约大学坦顿工程学院，纽约 11201，美国）

摘要：图像匹配导航技术是近年来自主导航领域的研究热点之一，但图像匹配算法的实时性却难以满足现实导航系统的需求。本文改进了传统线段提取算法，并引入了Delaunay三角剖分法，通过结合点线几何特征，减少了图像特征冗余。结合置信度准则对误差进行分析，完成匹配过程。仿真结果表明，本文算法在3°旋转并有尺度变化的情况下仍然能完成匹配，图像尺寸为256像素×256像素时匹配时间在0.5 s以内，适用于特征分布较多且实时性要求较高的自主导航系统。

关键词：图像匹配；导航；霍夫变换；Delaunay三角剖分；组合特征